PHOTOCATALYTIC BEHAVIOR OF GADOLINIA-CERIA MIXED OXIDES FOR LEAD (II) IONS' REMOVAL FROM WATER

Jiratchaya Ayawanna*

Received: January 09, 2017; Revised: March 03, 2017; Accepted: March 08, 2017

Abstract

The photocatalytic removal of Pb(II) ions from water by Gd_2O_3-CeO_2 mixed oxides was investigated. The heat treatment of the Gd_2O_3-CeO_2 particles affects the removal of Pb(II) ions accompanied with an absorption and a precipitation of Pb(II) ions. A partial dissolution of Gd_2O_3 was detected for the 2-phase mixture of Gd_2O_3-CeO_2 particles calcined at 1,000°C, which increases the pH-value of the Pb(II) solution and results in a $Pb(OH)_2$ precipitation, regardless of the photo-irradiation. The Gd_2O_3-CeO_2 particles calcined at 1,400°C form a solid solution Gd_2O_3-CeO_2 ($Ce_{0.9}Gd_{0.1}O_{1.95}$ or GDC) coexistent with CeO_2 particles (GDC-CeO_2), which decreases the pH of the Pb(II) solution and exhibits a more effective Pb(II) ion removal. A photoelectrodeposition of PbO_2 and a precipitation of $Pb(NO_3)_2$ are deposited on the surface of the mixture phase GDC-CeO_2 particles. The enhanced photocatalytic activity is supported by a strong photoluminescence signal, suggesting the fast transfer and efficient separation of photogenerated electron-hole pairs due to the formation of an interface between the solid solution GDC and CeO_2 particles.

Keywords: Cerium oxide, gadolinium oxide, semiconductor, photocatalysis, lead, wastewater

Introduction

Lead ion, i.e. Pb(II), is a toxic metal ion which can seriously damage the nervous system, kidneys, liver, and fundamental cellular processes in all living organisms (Fu and Wang, 2011). The Pb(II) ion is frequently found in industrial wastewater and corroded plumbing systems in public and private buildings. Treatments of Pb(II)-contaminated water can be performed by several techniques, e.g., chemical precipitation, ion exchange,

School of Ceramic Engineering, Institute of Engineering, Suranaree University of Technology, Nakhon Ratchasima, 30000, Thailand. Tel. 0-4422-4492; E-mail: jiratchaya@sut.ac.th
* *Corresponding author*

and adsorption process (Xiong *et al.*, 2011; Naushad, 2014), and recent studies suggest that heterogeneous photocatalysis with UV light is an effective method for the rapid removal of Pb(II) and other metal ions in aqueous solutions by utilizing oxidative and reductive mechanisms (Mishra *et al.*, 2007; Murruni *et al.*, 2007; Aman *et al.*, 2011; Lopez-Munoz *et al.*, 2011). The principle processes of heterogeneous photocatalysis are that, when photons illuminate on a semiconductor particle - typically Titanium dioxide (TiO_2)-based, an electron in the valence band (VB) is promoted to the conduction band (CB), which subsequently creates a hole in the VB. Then, the hole and an electron can either react with the adsorbed species to induce redox reactions (Litter, 1999), or recombine whether on the surface or in the bulk of the particle.

Cerium oxide (CeO_2) is a harmless oxide semiconductor that is well known in photocatalytic research for its effective photocatalytic degradation of organic pollutants in a region between near-UV and a part of the visible region (Magesh *et al.*, 2009; Paola *et al.*, 2012; Feng *et al.*, 2013). Although CeO_2 is a promising material for practical photocatalytic applications, the photocatalytic activity of CeO_2 is limited by fast recombination of the photoinduced electron and hole, and so interfacial transfer and consequent decomposition by photocatalytic reaction is less likely to occur (Yang *et al.*, 2014b; Phanichphant *et al.*, 2016). Gadolinium oxide (Gd_2O_3) has been reported to be a dopant in TiO_2 demonstrating the well-improved photocatalytic activity of the TiO_2 particles by reducing the recombination rate of the charge carriers for the photodegradation of organic dyes (Xu *et al.*, 2002, Farbod and Kajbafvala, 2013). Suppressing the recombination rate can also be achieved by incorporating CeO_2 with other semiconductors (Malecka *et al.*, 2007; Siriwong *et al.*, 2012).

Therefore, the potential of the photocatalyst Gd_2O_3-CeO_2 mixed oxide particles prepared at different temperatures for removal of Pb(II) ions in synthesized Pb(II)-polluted water has been studied. Utilization of the photocatalytic activity of the Gd_2O_3-CeO_2 system to eliminate toxic metallic ions, especially for Pb(II) ion in water, has been reported in this work.

Materials and Methods

A 5-mol% Gd_2O_3-CeO_2 mixed oxide is prepared by mixing a Gd_2O_3 powder and a CeO_2 powder (Nacalai Tesque Inc., Kyoto, Japan) in 2-Propanol using a planetary Pulverisette-7 micromill (Fritsch GmbH, Kastl-Utzenhofen, Germany) at a frequency of 1,600 rpm for 30 min. The milled mixture is then dried in an oven at 80°C for 4 h, and is later divided into 2 sets for separate calcination in the air under (1) 1000°C for 16 h, and (2) 1400°C for 5 h.

Fifty mg of the Gd_2O_3-CeO_2 particles is added into an aqueous solution of 30 ml of 1 $mmolL^{-1}$ (207 mgL^{-1}) $Pb(NO_3)_2$ (99.5%, Nacalai Tesque, Kyoto, Japan) for removal experiments. The photo–irradiation method is carried out for an external irradiation-type quartz cell containing a suspension sample. Each suspension is individually agitated at 500 rpm for 10, 30, 60, 120, and 180 min with a magnetic stirrer, and is also irradiated with a 200 W Hg-Xe lamp (L10852, LC8, Shimadzu Corporation, Tokyo, , Japan) having a wavelength of 200 nm. The non-irradiated experimental set is carried out on suspensions by stirring in dark conditions. The Gd_2O_3-CeO_2 particles in the Pb(II) solution are filtered out through a membrane filter (Type JGWP, Millipore, 0.2 μm aperture) and left overnight for 10 h before drying at 80°C.

Crystalline phases of the calcined Gd_2O_3-CeO_2 particles are identified with a RINT-2200HF X-ray diffractometer with Cu-Kα1 radiation λ = 1.540562 Å (Rigaku Corporation, Tokyo, Japan), powered at 40 kV and 30 mA. The 2θ scan is in a range between 20° and 90° with a step of 0.02° and a time-step of 1 s. A spectrofluorometer (FP-8500, JASCO International Co., Ltd., Hachioji, Japan) is used for recording luminescence spectra of the particles. A xenon lamp source with a wavelength of 360 nm is used as an excitation source for the photoluminescence.

Concentrations of Pb(II) ions residual in the solutions are measured by inductively coupled plasma atomic emission spectroscopy (ICPS-7510, Shimadzu Corporation, Tokyo, Japan). A standard calibration is carried out by using a 1,000 mgL^{-1} Pb(II) standard solution (Nacalai Tesque Inc., Kyoto, Japan) diluted to produce 1, 10, 50, 100, and 200 mgL^{-1} solutions.

The measured residual concentrations are later subtracted with the initial concentration of Pb(II) ions, resulting in the concentrations of the Pb(II) ion removal. Consequently, the difference of the removed concentrations between the UV-irradiated sample and the non-irradiated sample is an effective concentration of the removed Pb(II) ions.

After the removal experiment, the morphology of the Gd_2O_3-CeO_2 particles is visualized with a field emission-scanning electron microscope (FE-SEM SU8000, Hitachi Ltd., Tokyo, Japan) operating at 3 kV together with a scanning electron microscope (TM3000SEM, - Hitachi Ltd., Tokyo, Japan) operating at 15 kV. An elemental analysis is performed in situ with an electron probe microanalyzer (EPMA-1600, Shimadzu Corporation, Tokyo, Japan) coated with gold.

Results and Discussion

Pb(II) Ion Removal by the Gd_2O_3-CeO_2 Mixed Oxide Particles

The values from the tests of the effective Pb(II) removal that was affected solely by the photocatalytic reaction are shown in Table 1. Pure CeO_2 particles show the lowest efficiency, compared to calcined Gd_2O_3-CeO_2 particles. Gd_2O_3-CeO_2 particles that are calcined at higher temperatures exhibit a higher removal concentration; the particles calcined at 1400°C show the highest removal rate under photo-irradiation. However, a certain amount of Pb(II) ion removal was detected in the other samples despite an absence of the photo-irradiation. In Figure 1, the FE-SEM analysis reveals that there is a high contrast of lead (IV) oxide (PbO_2) deposits on the surface of the Gd_2O_3-

Table 1. Pb(II) ions removal concentration by calcined Gd_2O_3-CeO_2 mixed oxide particles

Calcination Temperature (°C)	Removal concentration ($mg \cdot L^{-1}$) after 180 min test		
	Photo-irradiation* (A)	Non-irradiation* (B)	Effective Values (A) – (B)
Pure CeO_2	5.0 ± 0.3	4.0 ± 0.9	1.0 ± 0.6
1000-16 h	158 ± 1.0	73 ± 0.6	85 ± 1.6
1400-5 h	186 ± 0.8	0.2 ± 0.1	185.8 ± 1.0

* Values from 3-times repeated experiments in 207 $mg \cdot L^{-1}$ Pb(II) solution

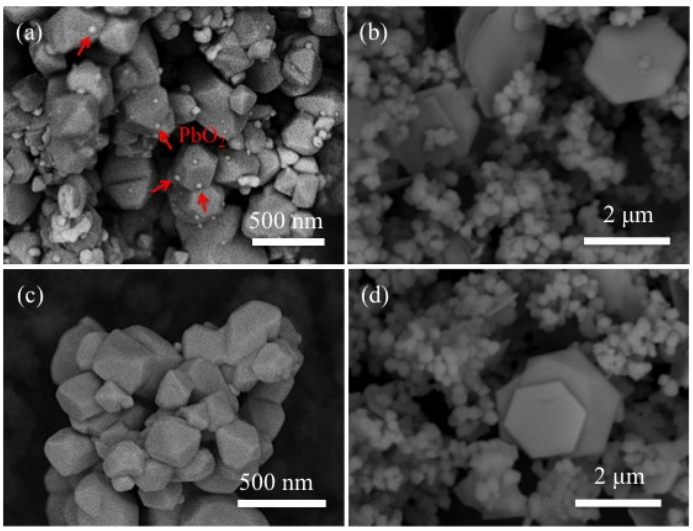

Figure 1. SEM images of Gd_2O_3-CeO_2 mixed oxide particles calcined at 1000°C for 16 h in the Pb(II) removal for 3 h: (a) and (b) with UV-irradiation, and (c) and (d) without irradiation

CeO_2 particles calcined at 1000°C after the removal under a UV-irradiation, as shown in Figure 1(a). Regardless of the radiation, $Pb(OH)_2$ having a hexagonal-like structure was detected in either the UV-irradiated (Figure 1(b)) or non-irradiated (Figure 1(d)) samples; this can clarify a certain activity for the removal of Pb(II) ions without the radiation as reported by Ayawanna *et al.* (2015). Dissolution of Gd_2O_3 in the Pb(II) solution during the tests gives hydroxyl ions resulting in an increase of the pH value from 5 to 7.2 in the systems regardless of photo-irradiation, as shown in Figure 2. Thus, $Pb(OH)_2$ is a product of the reaction between the Pb(II) ions and hydroxyl ions.

Figure 3 exhibits the amount of dissolved Gd(III) ions after the tests using the Gd_2O_3-CeO_2 particles calcined at 1000°C. The increase of dissolved Gd(III) ions and a deceleration of the removal of Pb(II) ions over the time are consistent with the change of the pH values, as shown in Figure 2. According to the X-ray diffraction (XRD) result in Figure 4, a Gd_2O_3 phase (Powder Diffraction File (PDF)# 03-065–3181) is separated from the CeO_2 major phase (PDF# 03-065-5923) in the Gd_2O_3-CeO_2 particles calcined at 1000°C. Introducing the 1000ºC-calcined Gd_2O_3-CeO_2 particles into the Pb(II) solution, which has a pH value around 5, results in a dissolution of Gd_2O_3.

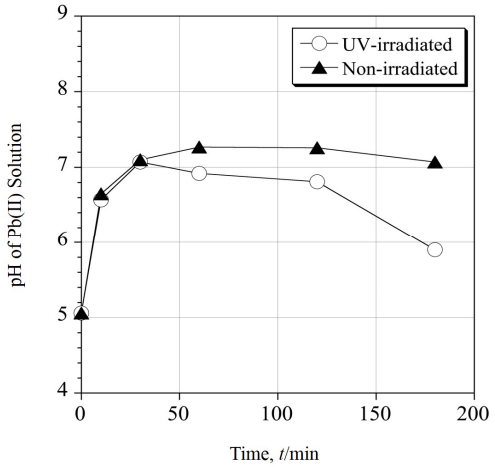

Figure 2. pH of Pb(II) solution after photocatalytic removal test by Gd_2O_3-CeO_2 mixed oxide particles calcined at 1000°C for 16 h

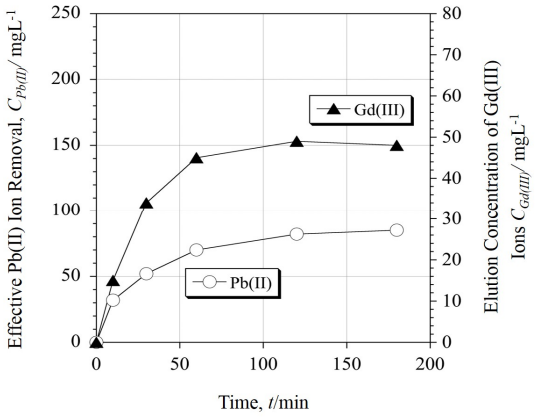

Figure 3. Effective removal concentration of Pb(II) ion by Gd_2O_3-CeO_2 mixed oxide particles calcined at 1000°C for 16 h in relation to the elution of Gd(III) ions

This is due to the fact that Gd_2O_3, as a lanthanide oxide, can simply be dissolved in an acidic solution having a pH value lower than 6.4 (Hyodo *et al.*, 2011). Thereby, an increase of the pH in the Pb(II) solution, as mentioned above, is likely due to a partial dissolution of Gd_2O_3 out of the 2-phase mixture of Gd_2O_3-CeO_2 calcined at 1000°C during the removal experiment. This result is in an agreement with the outcome of the study of Hemmer *et al.* (2012).

The XRD pattern in Figure 4(c) shows, however, that a Gd_2O_3 phase is not found in the Gd_2O_3-CeO_2 particles calcined at 1400°C. The diffracted peaks corresponding to a cubic $Ce_{0.9}Gd_{0.1}O_{1.95}$ phase (PDF# 01-075-0161) were obtained with the CeO_2 major phase, suggesting a formation of a partial solid solution between the Gd_2O_3-doped and CeO_2 nanoparticles (GDC). A descendent 422-peak shift in CeO_2 shown in Figure 5 suggests a substitution of larger Gd^{3+} ions for the lattice Ce^{4+} ions in the host lattice CeO_2 during the 1400°C calcination. The absence of dissolved Gd(III) ions and the increment of Pb(II) ion removal over the time shown in Figure 6 are in

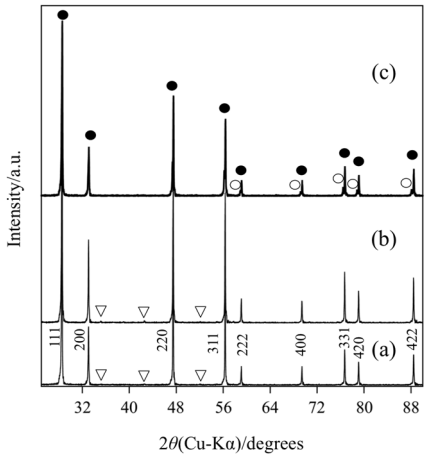

Figure 4. XRD patterns of Gd_2O_3-CeO_2 particles: (a) the as-mixed particles, and the calcined particles at (b) 1000°C for 16 h, and (c) 1400°C for 5 h (●; CeO_2, ▽; Gd_2O_3, ○; $Ce_{0.9}Gd_{0.1}O_{1.95}$, GDC)

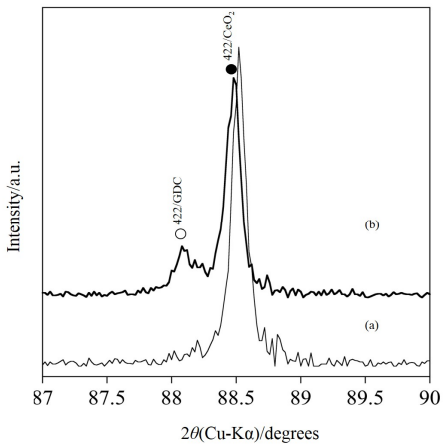

Figure 5. XRD patterns at high 2θ position of Gd_2O_3-CeO_2 mixed oxide particles: (a) the as-mixed particles and (b) the calcined particles at 1400°C for 5 h (●; CeO_2, ○; $Ce_{0.9}Gd_{0.1}O_{1.95}$, GDC)

agreement with the XRD result; that is, the 1400°C-calcined particles are $Ce_{0.9}Gd_{0.1}O_{1.95}$-CeO_2 having no Gd_2O_3. Therefore, when the $Ce_{0.9}Gd_{0.1}O_{1.95}$-CeO_2 is introduced into the Pb(II) solution, there is no Gd(III) ion found in the solution, and the outcome is only PbO_2 without $Pb(OH)_2$. Changes of the pH- values of the Pb(II) solution are insignificant during the experiment without the photo–irradiation, as shown in Figure 7. Consequently, the effective Pb(II) ion removal is increased with the reaction time, as shown in Figure 6, resulting in a decrease of pH values in the UV-irradiated sample.

FE-SEM images in Figure 8 reveal 2 different morphologies of deposits on the surface of the GDC-CeO_2 particles after the UV-irradiation (Figure 8(a)), whereas a clear surface is found in the case of the non-irradiated particles (Figure 8(b)). These indicate that both morphologies are yields of the photocatalytic Pb(II) ion removal process. The deposited PbO_2 particles are small and have a round shape. In addition, the pH value of the Pb(II) solution is lowered. This is in an agreement with the findings of a previous work on Pb(II) removal by TiO_2 reviewed by Murruni *et al.* (2007).

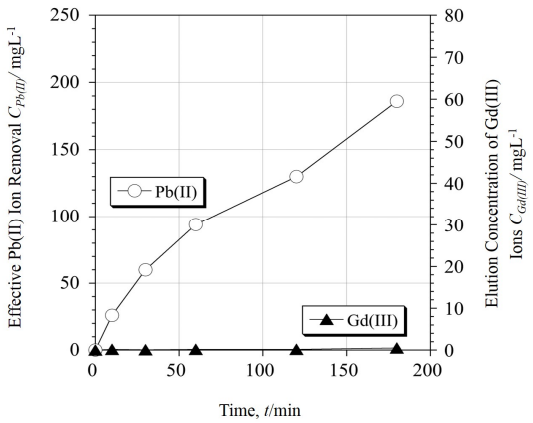

Figure 6. Effective removal concentration of Pb(II) ions by GDC-CeO_2 particles in relation to the elution of Gd(III) ions

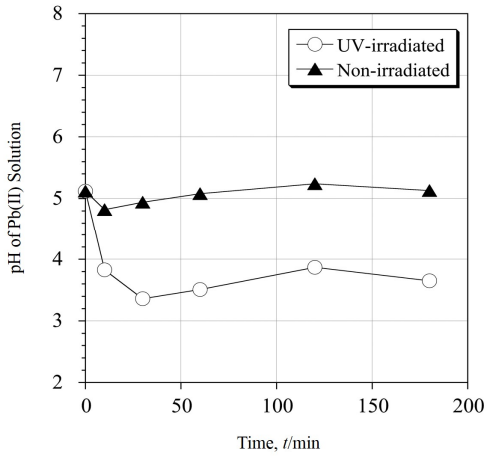

Figure 7. pH of Pb(II) solution after the photocatalytic removal test by GDC-CeO_2 particles

The other deposit has a cubical form, and is most likely a lead (II) nitrate ($Pb(NO_3)_2$) that can precipitate in an acidic solution. Ostanova *et al.* (2002) reveal that the solubility of $Pb(NO_3)_2$ in aqueous solutions of nitric acid (HNO_3) markedly decreases with an increase of the HNO_3 concentration, resulting in a recrystallization of $Pb(NO_3)_2$. Although HNO_3 is not used in this work, $Pb(NO_3)_2$ can be formed under the Pb(II) solution with a pH-value of 3.5 during the photocatalytic Pb(II) removal by the GDC-CeO_2 particles. Since the cubical $Pb(NO_3)_2$ crystal is easily dissolved in room-temperature water (Nowotny, 1986), the GDC-CeO_2 particles, after the removal test, were washed several times with distilled water prior to the FE–SEM examination. The micrograph in Figure 8(c) shows that the cubical $Pb(NO_3)_2$ deposits are completely removed from the surface of the GDC-CeO_2 particles, leaving only the PbO_2 that is insoluble in water.

Plausible Mechanism of Photoelectrodeposition PbO_2

A photoelectrodeposition of Pb(II) ions forming PbO_2 on the surface of the 2-phase mixture of the Gd_2O_3-CeO_2 particles calcined at 1000°C can occur when a photoexcitation generates electrons in the CB (e^-_{CB}) and holes in the VB (h^+_{VB}) of the Gd_2O_3-CeO_2 photocatalyst. The photo–generated electrons and holes can either recombine or transfer to surface adsorbed species, O_2 and Pb^{2+} respectively. The photocatalytic reaction is illustrated in Figure 9. A Gd_2O_3 phase inside a CeO_2 matrix can serve as an electron trap since the energy level of Gd_2O_3 is lower than the CB of CeO_2. However, a half–filled electronic configuration of Gd^{3+} is changed from a high spin state to a highly unstable low spin state when the Gd^{3+} lattice traps the electron (Saif *et al.*, 2014). As a result, a Gd^{3+} ion has to release the electron to the surface-adsorbed oxygen molecule, and subsequently restores to

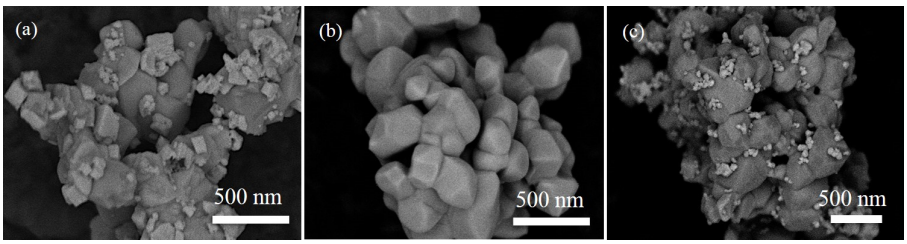

Figure 8. SEM images of GDC-CeO_2 particles after Pb(II) ions removal for 3 h: (a) with UV-irradiation, (b) without irradiation, and (c) UV-irradiated sample after water washing

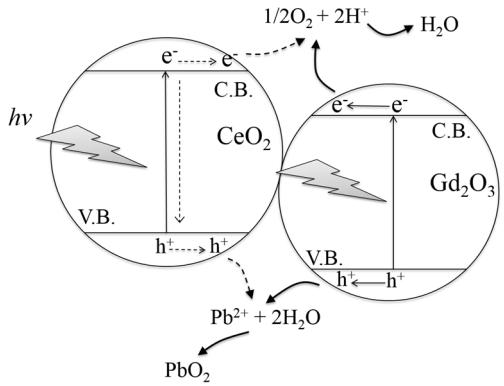

Figure 9. Schematic diagram showing proposed mechanism for electron-hole transfer between the Gd_2O_3-CeO_2 interfaces

the stable half-filled electronic configuration. The adsorbed oxygen is thus an electron acceptor, leading to a reduction reaction. A Pb(II) ion is simultaneously oxidized by a photogenerated hole, and reacts to the water molecule, resulting in PbO_2. This reaction occurs at the contact area between Gd_2O_3 and CeO_2 where the electrons and holes can approach for the oxidative reaction (Horvath and Voros, 2000).

In the case of the solid solution phase mixture of GDC-CeO_2 particles calcined at 1400°C, the photoelectrodeposition of Pb(II) ions is most likely to be effective at an interface between either the $Ce_{0.9}Gd_{0.1}O_{1.95}$ solid solution particle or the GDC and CeO_2 particle. GDC and CeO_2 can form a p-n heterojunction as shown in Figure 10, where GDC acts as the p-type and CeO_2 is the n-type (Ayawanna *et al.*, 2015). Holes from GDC will transfer to CeO_2, while electrons will diffuse from CeO_2 to GDC, owing to the concentration gradient of charge carriers (Figure 10(a)). Simultaneously, an electric field is built at the interface of the heterojunctions, having a field direction from CeO_2 toward GDC (Yang *et al.*, 2014a). During the photocatalytic process by GDC-CeO_2 particles as demonstrated in Figure 10(b), both CeO_2 and GDC are excited by photons, and subsequently the same number of electrons and holes are generated in the CB and the VB, respectively. The photogenerated electrons in GDC are quickly transferred to the CB of CeO_2 and, at the same time, the photogenerated holes in CeO_2 are transferred to the VB of the GDC, resulting in an efficient separation of the photogenerated charge carriers. As a consequence, the resultant holes in the VB of the GDC can oxidize Pb^{2+} yielding PbO_2, and simultaneously the resultant electrons in the CB of CeO_2 are transferred to O_2 molecules, located at a surface of the heterojunctions.

Photoluminescent Properties of Gd_2O_3-CeO_2 Photocatalyst

When a CeO_2 lattice is doped by 2 Gd^{3+} ions, there is a replacement of Ce^{4+} by Gd^{3+}, resulting in an oxygen vacancy. The resultant oxygen vacancy is then paired with Gd^{3+}, creating $(Gd^{3+} - V_o^{\cdot\cdot})^{\cdot}$. However, the association energy of $(Gd^{3+} - V_o^{\cdot\cdot})^{\cdot}$ is the lowest among all trivalent lanthanide dopants to dope in CeO_2 and, therefore, Gd^{3+} tends to leave $V_o^{\cdot\cdot}$, which resembles an oxygen–vacancy generator (Wei *et al.*, 2009). The abandoned $V_o^{\cdot\cdot}$ are attractive to photo-generated electrons via the electrostatic force, creating bound states or, in another word, excitons. These excitons are responsible

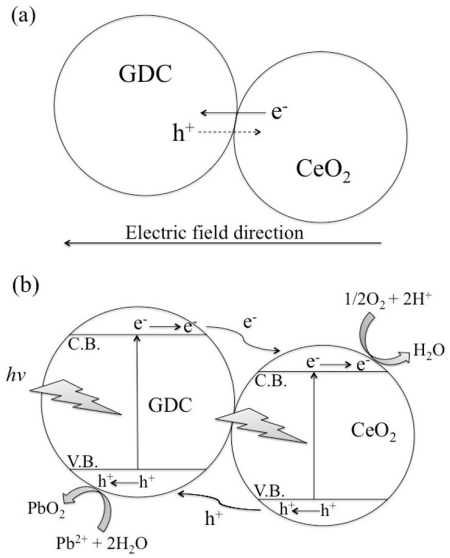

Figure 10. Schematic diagram showing proposed mechanism for (a) electron-hole transfer between the GDC-CeO_2 interfaces and (b) the photoelectrodeposition of Pb (II) ion on the surface of the GDC-CeO_2 particle

for the photoluminescent (PL) spectrum shown in Figure 11.

UV-VIS spectroscopy was used to speculate emission wavelengths in the UV range, and finds no emission at the wavelength of 380 nm, which corresponds to the absorption threshold of Gd_2O_3-CeO_2. In another PL measurement (not shown here), which is on CeO_2-doped with La^{3+}, the emission spectrum resembles the Gd^{3+} dopant (Choudhury and Choudhury, 2012). Therefore, the emission spectrum is not a dopant-type dependency, but there are excitons - the result of oxygen-vacancy and photo–generated electrons (Wang *et al.*, 2007).

In Figure 11, the highest PL intensity spectrum is found in the case of the GDC-CeO_2, compared to the 2-phase Gd_2O_3-CeO_2 and pure CeO_2. This is because the high content of surface oxygen vacancies can easily bind the photogenerated electrons to form excitons, and suppress the recombination of electrons and holes (Choudhury and Choudhury, 2012; Liqiang *et al.*, 2006). Therefore, the enhanced photocatalytic activity of GDC-CeO_2 is caused by effectively restraining the recombination of photogenerated electron-hole pairs.

Conclusions

Gd_2O_3-CeO_2 mixed oxide photocatalyst particles show potential in the removal of Pb(II) ions from water. The removal of Pb(II) ions by the 2-phase mixture of Gd_2O_3-CeO_2 photocatalysts accompanies the photoelectrodeposition of Pb(II) ions by the oxidation reaction to PbO_2 and a precipitation of $Pb(OH)_2$ regardless of photo-irradiation. Simultaneously, a photoelectrode-position of PbO_2 and $Pb(NO_3)_2$ deposits occurs on the surface of the solid solution phase mixture of $Ce_{0.9}Gd_{0.1}O_{1.95}$-CeO_2 photocatalyst particles. A strong photoluminescent band-emission signal suggests a high efficiency of photogenerated charge separation in the solid solution phase mixture of $Ce_{0.9}Gd_{0.1}O_{1.95}$-CeO_2, leading to more effective photocatalytic removal of Pb(II) ions compared to the 2-phase mixture of Gd_2O_3-CeO_2 particles. The formation of an interface between the solid solution $Ce_{0.9}Gd_{0.1}O_{1.95}$ phase and CeO_2 as a p-n heterojunction can prolong the recombination of the electrons and holes, allowing the easier transfer of photogenerated electron-hole pairs for the oxidation reaction of Pb(II) ions. The outcome of this study encourages industrial enterprises and opens an opportunity to utilize Gd_2O_3-CeO_2 mixed oxides as a catalyst for photocatalytic removal of heavy metal ions in polluted water.

Acknowledgements

This work was financially supported by the Japanese Government Research Fund, (#23651066). The author would also like to acknowledge Professor Kazunori Sato from

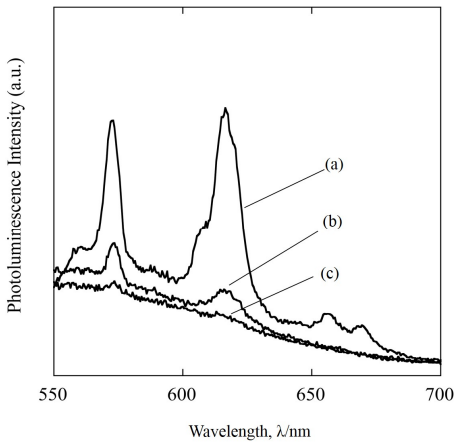

Figure 11. PL spectra of (a) GDC-CeO_2 particles and (b) Gd_2O_3-CeO_2 particles in comparison to (c) CeO_2 particles

Nagaoka University of Technology and Suranaree University of Technology whose assistance is highly appreciated.

References

Aman, N., Mishra, T., Hait, J., and Jana, R.K. (2011). Simultaneous photoreductive removal of copper (II) and selenium (IV) under visible light over spherical binary oxide photocatalyst. J. Hazard. Mater., 186:360-366.

Ayawanna, J., Teoh, W., Niratisairak, S., and Sato, K. (2015). Gadolinia-modified ceria photocatalyst for removal of lead (II) ions from aqueous solutions. Mat. Sci. Semicon. Proc., 40:136-139.

Choudhury, B. and Choudhury, A. (2012). Ce^{3+} and oxygen vacancy mediated tuning of structural and optical properties of CeO_2 nanoparticles. Mater. Chem. Phys., 131:666-671.

Farbod, M. and Kajbafvala, M. (2013). Effect of nanoparticle surface modification on the adsorption-enhanced photocatalysis of Gd/TiO_2 nanocomposite. Powder Technol., 239:434-440.

Feng, T., Wang, X., and Feng, G. (2013). Synthesis of novel CeO_2 microspheres with enhanced solar light photocatalytic properties. Mater. Lett., 100:36-39.

Fu, F. and Wang, Q. (2011). Removal of heavy metal ions from wastewaters: A review. J. Environ. Manage., 92:407-418.

Hemmer, E., Venkatachalam, N., Hyodo, H., and Soga, K. (2012). The role of pH in PEG-b-PAAc modification of gadolinium oxide nanostructures for biomedical applications. Adv. Mater. Sci. Eng., 1-15.

Horvath, O. and Voros, J. (2000). Photoinduced electron ejection from trihydroxoplumbate(II) in alkaline aqueous solution. Inorg. Chem. Comm., 3:191-193.

Hyodo, H., Sato, N., Kitano, K., and Soga, K. (2011). Surface modification of ceramic nanophosphors by atmospheric pressure plasma. J. Photopolym. Sci. Tec., 24:429-433.

Liqiang, J., Yichun, Q., Baiqi, W., Shudan, L., Baojiang, J., Libin, Y., Wei, F., Honggang, F., and Jiazhong, S. (2006). Review of photoluminescence performance of nano-sized semiconductor materials and its relationships with photocatalytic activity. Sol. Energ. Mat. Sol. C., 90:1773-1787.

Litter, M. I. (1999). Heterogeneous photocatalysis transition metal ions in photocatalytic systems. Appl. Catal. B-Environ., 23:89-114.

Lopez-Munoz, M.J., Aguado, J., Arencibia, A., and Pascual, R. (2011). Mercury removal from aqueous solutions of $HgCl_2$ by heterogeneous photocatalysis with TiO_2. Appl. Catal. B-Environ., 104:220-228.

Magesh, G., Viswanathan, B., Viswannath, R.P., and Varadarajan, T.K. (2009). Photocatalytic behavior of CeO_2-TiO_2 system for the degradation of methylene blue. Indian J. Chem. A., 48:480-488.

Malecka, M.A., Kepinski, L., and Mista, W. (2007). Structure evolution of nanocrystalline CeO_2 and $CeLnO_x$ mixed oxides (Ln = Pr, Tb, Lu) in O_2 and H_2 atmosphere and their catalytic activity in soot combustion. Appl. Catal. B-Environ., 74(3-4):290-298.

Mishra, T., Hait, J., Aman, N., Jana, R.K., and Chakravarty, S. (2007). Effect of UV and visible light on photocatalytic reduction of lead and cadmium over titania based binary oxide materials. J. Colloid Interf. Sci., 316:80-84.

Murruni, L., Leyva, G., and Litter, M.I. (2007). Photocatalytic removal of Pb(II) over TiO_2 and Pt-TiO_2 powders. Catal. Today, 129:127-135.

Naushad, M. (2014). Surfactant assisted nano-composite cation exchanger: Development, characterization and applications for the removal of toxic Pb^{2+} from aqueous medium. Chem. Eng. J., 235:100-108.

Nowotny, H. (1986). Structure refinement of lead nitrate. Acta. Crystallogr. C, 42:133-135.

Ostanova, S.V., Chubarov, A.V., Drozdov, S.V., Patrushev, V.V., and Tatarenko, V.V. (2002). Solubility of lead nitrate in aqueous solutions of nitric acid and zinc nitrate. Russ. J. Appl. Chem., 75:1024-1025.

Paola, A.D., Garcia-Lopez, E., Marci, G., and Palmisano, L. (2012). A survey of photocatalytic materials for environmental remediation. J. Hazard Mater., 211-212:3-29.

Phanichphant, S., Nakaruk, A., and Channei, D. (2016). Photocatalytic activity of the binary composite CeO_2/SiO_2 for degradation of dye. Appl. Surf. Sci., 387:214-220.

Saif, M., Aboul-Fotouh, S.M.K., El-Molla, S.A., Ibrahim, M.M., and Ismail, L.F.M. (2014). Evaluation of the photocatalytic activity of Ln^{3+}-TiO_2 nanomaterial using fluorescence technique for real wastewater treatment. Spectrochim. Acta A, 128:153-162.

Siriwong, C., Wetchakun, N., Inceesungvorn, B., Channei, D., Samerjai, T., and Phanichphant, S. (2012). Doped-metal oxide nanoparticles for use as photocatalysts. Prog. Cryst. Growth Ch., 58:145-163.

Wang, Z., Quan, Z., and Lin, J. (2007). Remarkable changes in the optical properties of CeO_2 nanocrystals induced by lanthanide ions doping. Inorg. Chem., 46(13):5237-5242.

Wei, X., Pan, W., Cheng, L., and Li, B. (2009). Atomistic calculation of association energy in doped ceria. Solid State Ionics, 180:13-17.

Xiong, L., Chen, C., Chen, Q., and J. Ni. (2011). Adsorption of Pb(II) and Cd(II) from aqueous solutions using titanate nanotubes prepared via hydrothermal method. J. Hazard Mater., 189:741-748.

Xu, A.W., Gao, Y., and Liu, H.Q. (2002). The preparation, characterization, and their photocatalytic activities of rare-earth-doped TiO_2 nanoparticles. J. Catal., 207:151-157.

Yang, Z.-M., Hou, S.-C., Huang, G.-F., Duan, H.-G., and Huang, W.-Q. (2014a). Electrospinning preparation of p-type NiO/n-type CeO_2 heterojunctions with enhanced photocatalytic activity. Mater. Lett., 133:109-112.

Yang, Z.-M., Huang, G.-F., Huang, W.-Q., Wei, J.-M., Yan, X.-G., Liu, Y.-Y., Jiao, C., Wan, Z., and Pan, A. (2014b). Novel Ag_3PO_4/CeO_2 composite with high efficiency and stability for photocatalytic applications. J. Mater. Chem. A, 2:1750-1756.